Supplementary Information

Cyclic Production of Biocompatible Few-layer Graphene Ink with In-line Shear-Mixing for Inkjet-Printed Electrodes and Li-ion Energy Storage

Tian Carey[1,2], Abdelnour Alhourani[3], Ruiyuan Tian[2], Shayan Seyedin[4], Adrees Arbab[1], Jack Maughan[2], Lidija Šiller[4], Dominik Horvath[2], Adam Kelly[2], Harneet Kaur[2], Eoin Caffrey[2], Jong M. Kim[1], Hanne R. Hagland[3], Jonathan N. Coleman[2*]*

[1]Cambridge Graphene Center, Department of Engineering, University of Cambridge, UK

[2]CRANN and AMBER Research Centres, Trinity College Dublin, Dublin 2, Ireland

[3]Department of Chemistry, Bioscience and Environmental Engineering, University of Stavanger, Norway

[4]School of Engineering, Newcastle University, UK

*Correspondence and requests for materials should be addressed to T.C. (tian.carey@cantab.net) and J.C. (colemaj@tcd.ie)

Supplementary Note 1

Comparison between shear mixing methods

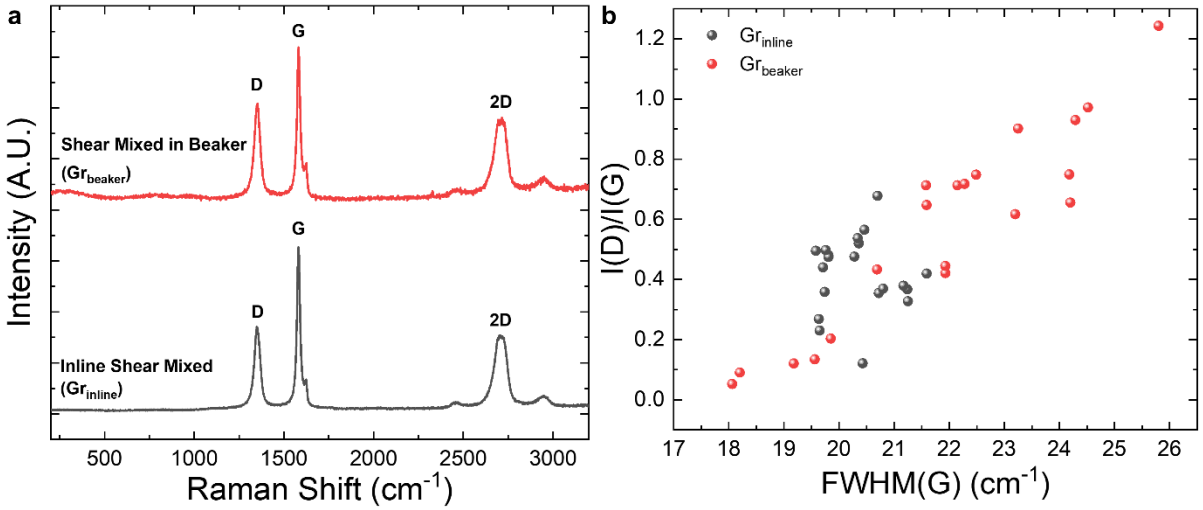

Supplementary Figure 1: a) Raman spectrum for shear mixed graphene in a beaker for 18 hours (red) and spectrum of inline-shear-mixed graphene for 6000 cycles, 18 hours (black). b) The *I(D)/I(G)* ratio as a function of the *FWHM(G)*.

For this study, we make two different graphene inks. A graphene dispersion is prepared by conventional shear mixing in a beaker. We mix graphite flakes (Imerys, 100 mg ml^{-1}) with SDC 5 mg ml^{-1} in deionized water and shear at 8000 rpm for 18 hours (Silverson high-shear mixer, rotor gap-stator of 300 μm and a rotor diameter of 31.1 mm). The dispersion is then centrifuged (Sorvall WX100 mounting a TH-641 swinging bucket rotor) at 1 k rpm (20 min) to make the graphene ink (Gr$_{beaker}$). A second ink is prepared using an inline attachment to the shear mixer as described in the main text (Silverson, rotor gap-stator of 300 μm and a rotor diameter of 31.1 mm). We mix graphite flakes (Imerys, 100 mg ml^{-1}) with SDC 5 mg ml^{-1} in deionized water and shear at 8000 rpm for 18 hours to make a graphene ink with high c ~ 100 mg ml^{-1} (Gr$_{inline}$). A volume of 1000ml is processed for Gr$_{beaker}$ and Gr$_{inline}$.

We undertake Raman spectroscopy on drop cast films of each ink on Si/SiO$_2$. In supplementary figure 1a Gr$_{beaker}$ has a D, G, and single Lorentzian fit of the 2D peak indicating electronically decoupled graphene. Similarly, Gr$_{inline}$ (black curve) also displays these peaks. In

supplementary figure 1b the *FWHM(G)* is broad for Gr_{beaker}, ranging from 18 cm^{-1} to 26 cm^{-1} suggesting a more disordered material. Similarly, the *I(D)/I(G)* ratio for the shear mixed material in a beaker is broad, ranging from values of 0.05 to 1.2, suggesting a defective material.[1] We plot the *FWHM(G)* vs. *I(D)/I(G)* in supplementary figure 1b and find a direct correlation which we attribute to in-plane defects.[1]

Supplementary Note 2

Calculation of the Reynolds number

The Reynolds number ($Re = \rho v L\ \eta^{-1}$) can be defined as the ratio between the frictional force, and the force of inertia, where ρ is the liquid density, v is the liquid velocity, L is the characteristic length and η is the liquid viscosity. We estimate v from the equation, $v = 2\pi D/2 \times RPM/60 \simeq 10$ m s^{-1}, where D is the diameter of the rotor blade. The value for v is similar to estimations from simulations of the liquid velocity around a rotor blade.[2] We estimate the liquid density near that of deionised water $\rho \sim 1000$ kg m^{-3}. We define L as the system's volume ($\pi r^2 h$, assuming a cylinder shape) divided by the surface area perpendicular to the liquid flow (πr^2). Therefore we can estimate $L \sim \pi r^2 h / \pi r^2 \sim h$, where h is the height of the container where the exfoliation of the graphene flakes is taking place. Similar definitions for L of a 3-dimensional system have been used to calculate L in the combustion chamber of rocket engines.[3] The height of our beaker is ~ 13 cm while the height of the inline shear mixing chamber is ~ 6 cm. Therefore, we can calculate $Re_{beaker} = \rho v L/\eta \sim 1.3 \times 10^6$ and $Re_{inline} \sim 6 \times 10^5$. In both systems $Re > 10^4$, indicating that there is turbulent liquid flow.[4] We attribute the reduction of in-plane defects found in our in-line shear mixed samples to the reduction in *Re*, which also suggests that reducing *Re* is desirable to increase the graphene quality and reduce defects. It is possible that greater hydrodynamic stress is generated in higher *Re*, which creates topological defects in the graphene flakes. For example, Bracamonte et. al. has exfoliated graphene flakes by bath sonication and has demonstrated that topological defects are introduced after 2 hours due to

hydrodynamic stress.[5] Therefore, it is likely that increasing $Re > 10^6$ during exfoliation can damage the graphene flakes and induce topological defects.[5]

The σ of Gr_{inline} and Gr_{beaker} is similar $\sigma \sim 10^3$ S/m, which is surprising since centrifugation is not undertaken on Gr_{inline}. We attribute the similar σ to the reduction of defects Gr_{inline}, in agreement with our Raman spectroscopy measurements. The σ of Gr_{inline} can be increased further with centrifugation reaching $\sigma \sim 5 \times 10^3$ S/m with similar centrifugation conditions to Gr_{beaker}. Typically inks with c ~ 1 mg ml^{-1} can only be made by conventional shear mixing in a beaker, while the inline system produces an ink with 100 times the concentration c ~ 100 mg ml^{-1} in the same time (18 hours). Therefore the inline shear mixing process offers a route to scale graphene production while maintaining a high σ and graphene quality, free of basal plane defects.

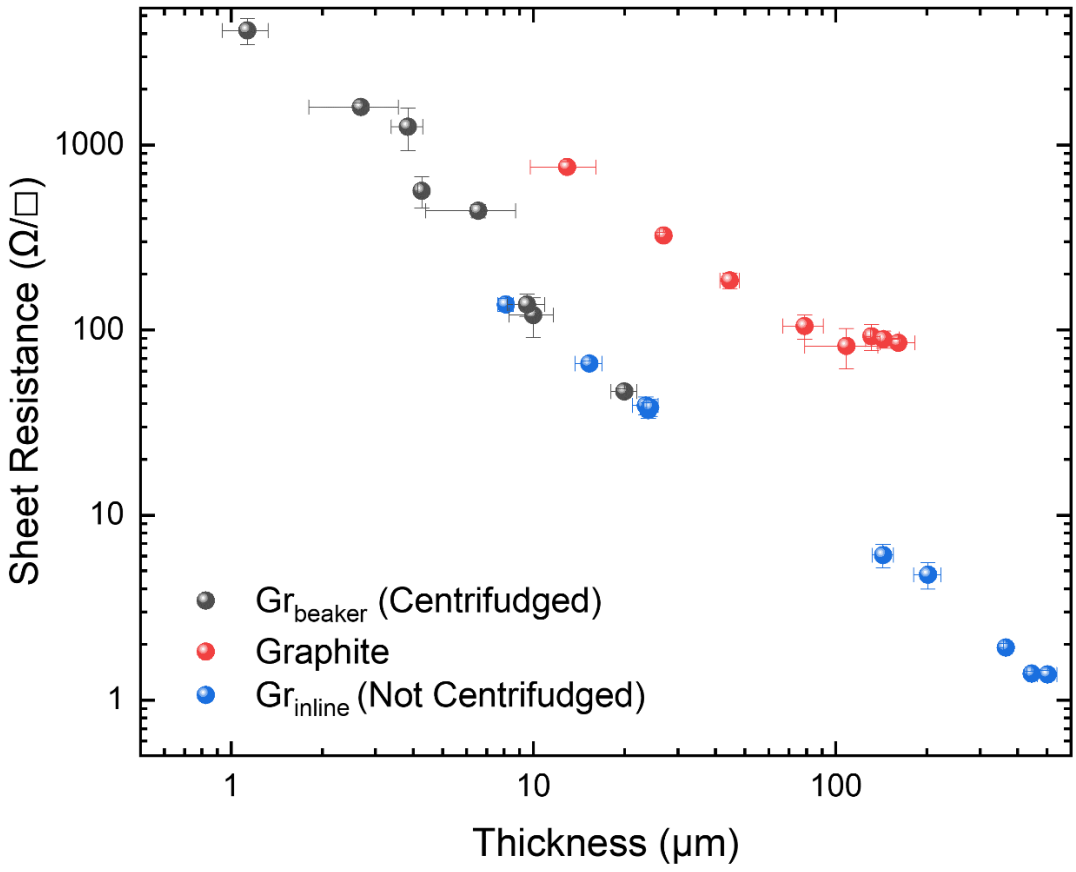

Supplementary Figure 2: **Electrical Properties Comparison between Gr_{inline}, Gr_{beaker} and Graphite**. Sheet resistance as a function of film thickness for the centrifuged shear mixed graphene after 18 hours of processing (Gr_{beaker}), starting graphite and uncentrifudged, unannealed 6000 cycles inline shear mixed material (Gr_{inline}). Error was calculated by SDOM.

Supplementary Note 3

XPS survey: Examination of Sodium, Carbon and Oxygen Content

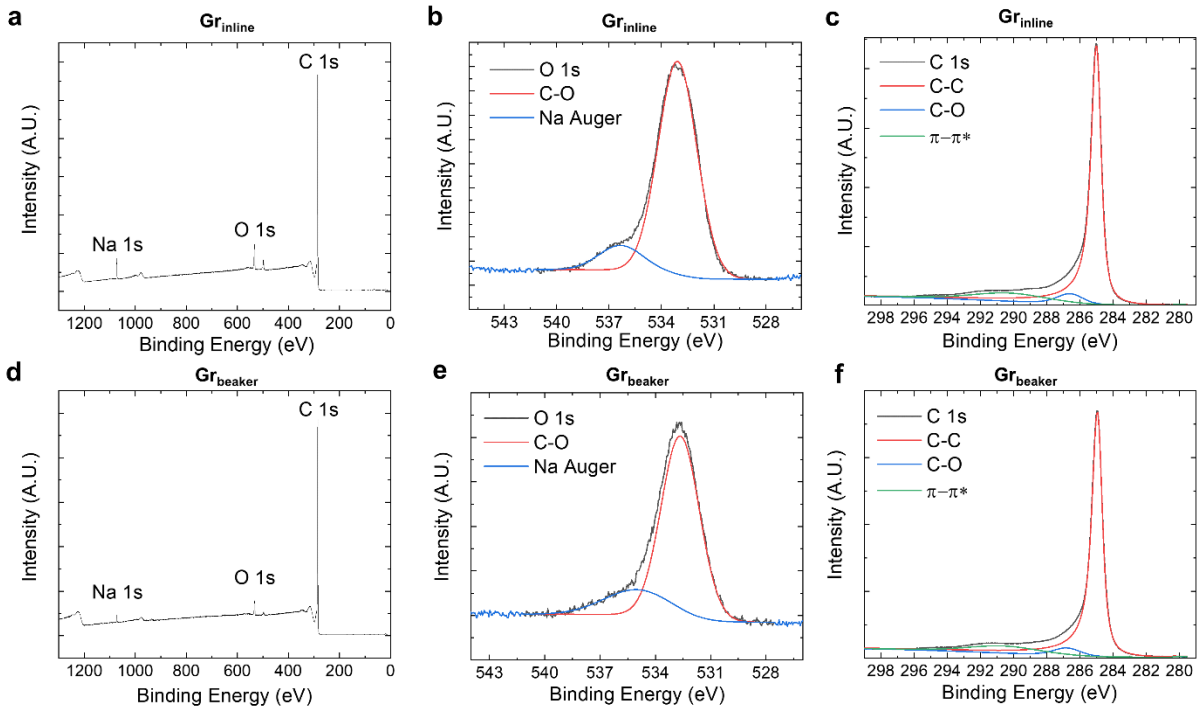

Supplementary Figure 3: **Elemental examination of Gr_{beaker} and Gr_{inline}.** a) XPS survey spectra b) XPS O 1s spectra and c) XPS C1s spectra of inline (6000 Cycles, 18 hours) graphene. d) XPS survey spectra e) XPS O 1s spectra and f) XPS C1s spectra of shear mixed graphene (processed for 18 hours).

We use X-ray photoelectron spectroscopy (XPS) analysis to investigate the oxygen and sodium content in Gr_{inline} and Gr_{beaker}. The XPS survey spectra (Supplementary figure 3a and 3d) shows very high carbon content (93 - 95 at.%), low oxygen content (<6% at.%) and sodium content (~1-2 at.%) for both Gr_{beaker} and Gr_{inline}. We attribute the sodium to residual SDC surfactant.

The Gr_{inline} sample shows a slightly higher oxygen content (5.7 ± 0.1 at.%) than Gr_{beaker} (3.6 ± 0.2 at.%). The relatively low oxygen content in both samples and the position of the main peak in O 1s spectra at ~533 eV (Supplementary Figure 3b and 3e) suggest C-O component dominance over C=O. The Gr_{inline} also shows a slightly higher sodium content (1.8 ± 0.02 at.%) than Gr_{beaker} (0.6 ± 0.04 at.%), which we attribute to the centrifugation step in Gr_{beaker} which could remove some of the surfactant. Investigation of the high-resolution XPS spectra (Figure 3c and 3f) for carbon 1s reveals a high contribution (~79-82 at.%, ~94 at.% if the π-π* contribution is included)[6] of sp^2 carbon component (peak at ~285 eV) for both Gr_{inline} (79 at.%) and Gr_{beaker} (82 at.%) samples, indictive of the hexagonal lattice structure. The satellite peak (π-π*) contribution, corresponding to the broad peak at ~290 eV is observed for both Gr_{inline} (15 at.%) and Gr_{beaker} (13 at.%). The π-π* satellite peak is a characteristic feature of sp^2 hybridisation of carbon.[7] The π-π* transition occurs due to the delocalisation of the π-electrons in the carbon aromatic ring.[8] To compare the π-π* transition in Gr_{inline} and Gr_{beaker} we use the ratio of the intensity of π-π* peak ($I_{\pi-\pi^*}$) to the intensity of the C-C peak (I_{C-C}). [9]We observe that the π-π* peak is more pronounced in Gr_{inline} ($I_{\pi-\pi^*}/I_{C-C}$ ~ 0.19) than Gr_{beaker} ($I_{\pi-\pi^*}/I_{C-C}$ ~ 0.15), suggesting that Gr_{inline} should have a higher conductivity.[10] In general, the more pronounced π-π* satellite peak, the greater the degree of sp^2 bonding. [11]

Supplementary Note 4

Toxicity of surfactant stabilisation agent

The cytotoxicity of sodium deoxycholate (SDC) in HUVECs and SW948 cells was assessed using CCK8 viability assay. Concentrations of 0.601 to 38.5 μg ml^{-1} of SDC were added to the cells for 48 hours to correspond to the SDC exposure expected from the biocompatibility testing in figure 7 of the main text. We observed no dose-dependent toxicity in either cell line up to 48 hours (supplementary figure 4).

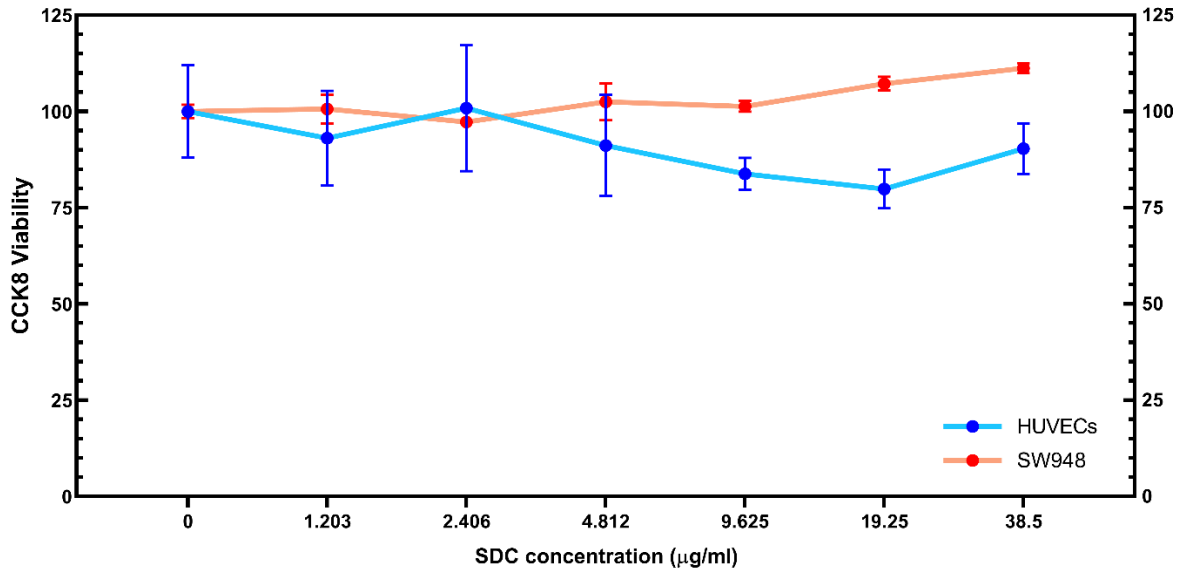

Supplementary Figure 4: **Surfactant toxicity assessment in human cell lines.** Cellular viability of HUVECs and SW948 cells after 48 hours of sodium deoxycholate (SDC) exposure (N=3 ±SD).

Supplementary Note 5

XRD Characterisation

X-ray diffraction (XRD) analysis was undertaken on Gr_{beaker} and Gr_{inline} after drying the dispersions (Supplementary Figure 5). The spectra show the presence of graphitic carbon signals, which include a sharp and high intensity (002) peak at $2\theta \sim 26.5°$ and additional (100), (101), (004), (110), and (112) peaks. These peaks match the graphite's XRD pattern suggested by powder diffraction (Crystallography Open Database, Reference Pattern 96-901-1578). This result indicates the liquid phase exfoliation process minimised defects compared to disorder seen in graphene oxide or reduced graphene oxide samples.[12]

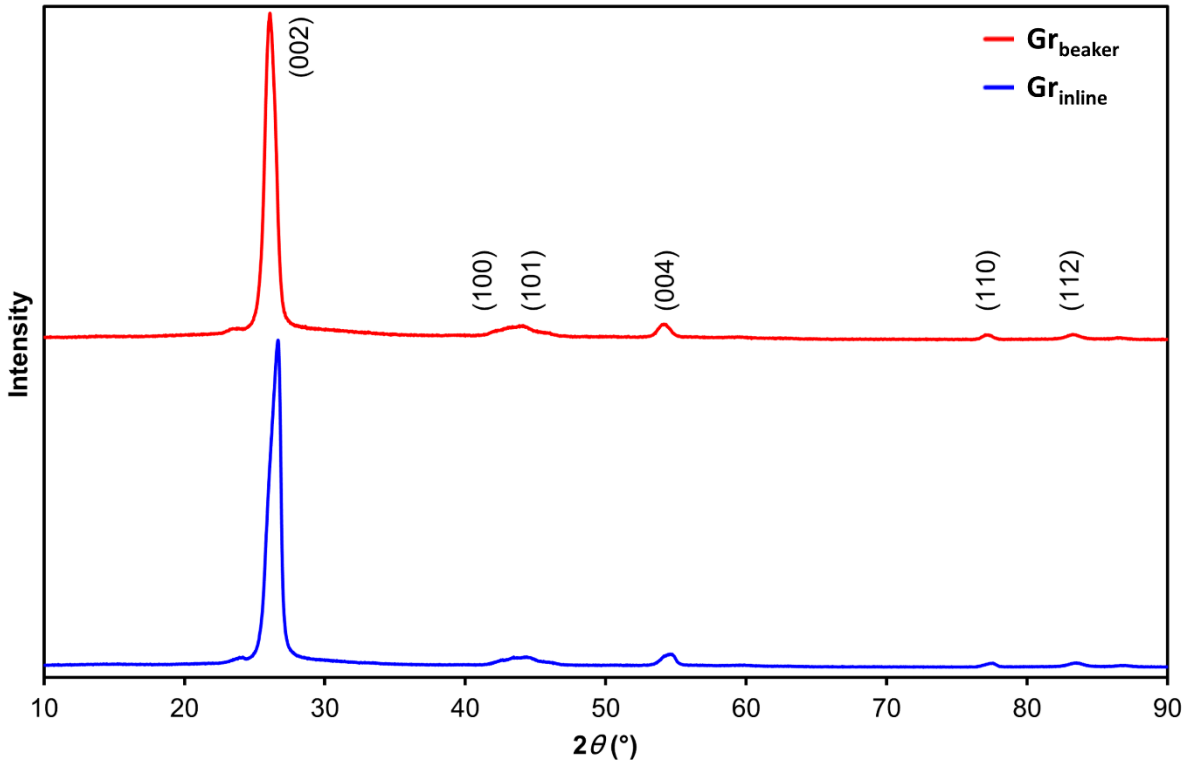

Supplementary Figure 5: **Examination of flake disorder**, XRD spectra of graphene dispersions prepared using shear mixing in a beaker for 18 hours and by inline shear mixing for 6000 cycles (18 hours).

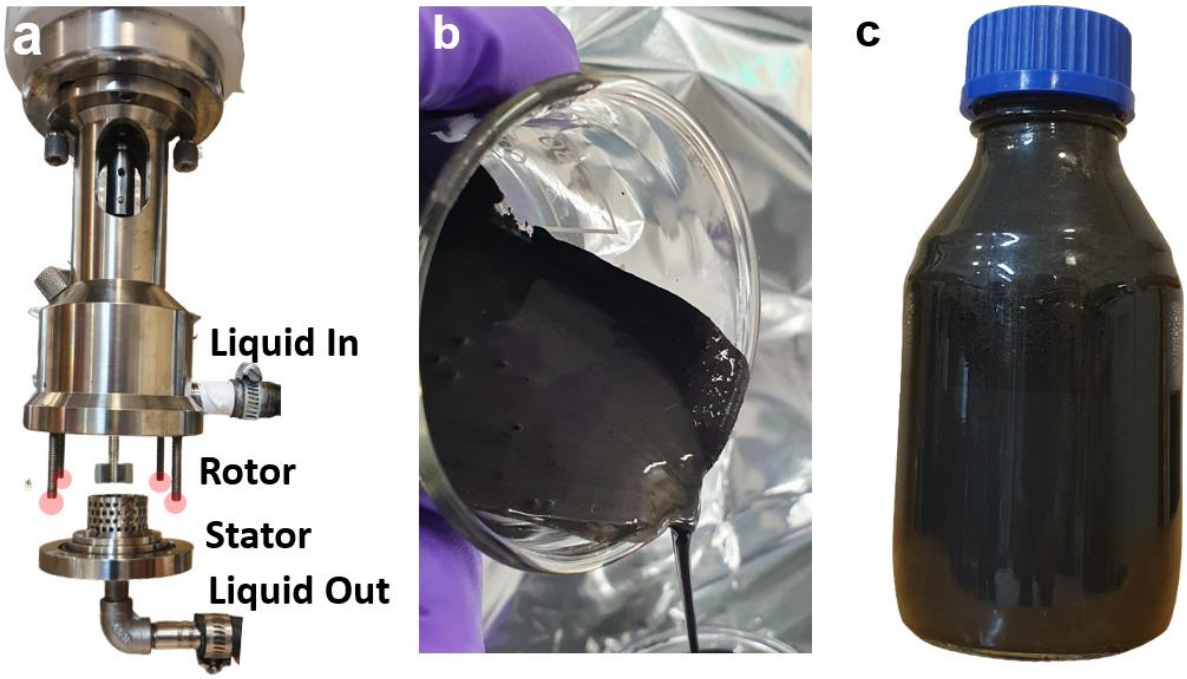

Supplementary Figure 6: **Schematics of experimental set-up and ink produced** a) Expanded view of the in-line shear mixer attachment. The components such as the rotor and

stator have been photoshopped into place for the purpose of illustration as they are typically out of view and enclosed. Four screws would be attached to the thread (shown by the red circles) to enclose the system in combination with an O-ring on the bottom of the stator to seal the system. b) Example of the 6000 cycles graphene ink ($c \sim 100$ mg ml^{-1}) being poured out of a beaker. c) Example of 500 ml of the 6000 cycles graphene ink.

Supplementary Note 6

We make two dispersions, 200 µg ml^{-1} of 6000 cycles graphene with cell culture media (as defined in the main text) and 200 µg ml^{-1} of 6000 cycles graphene with cell culture media without foetal bovine serum (FBS) added. Both dispersions are sonicated briefly (~2 min) to disperse the graphene flakes. The dispersions are left in a glass vial placed in a fume hood to aggregate over a 48-hour period and are gently shaken before imaging. In supplementary figure 7a we observe the presence of foetal bovine serum (FBS) prevents the graphene flakes from aggregating in the culture media, indicated by the presence of graphene flakes measuring < 2 µm in length as expected. Conversely, the graphene dispersed in cell culture media without FBS displays large aggregates between 10-20 µm in length indicating agglomeration of the graphene flakes. Similar graphene flake stability due to FBS was previously reported with graphene oxide (GO) flakes.[13]

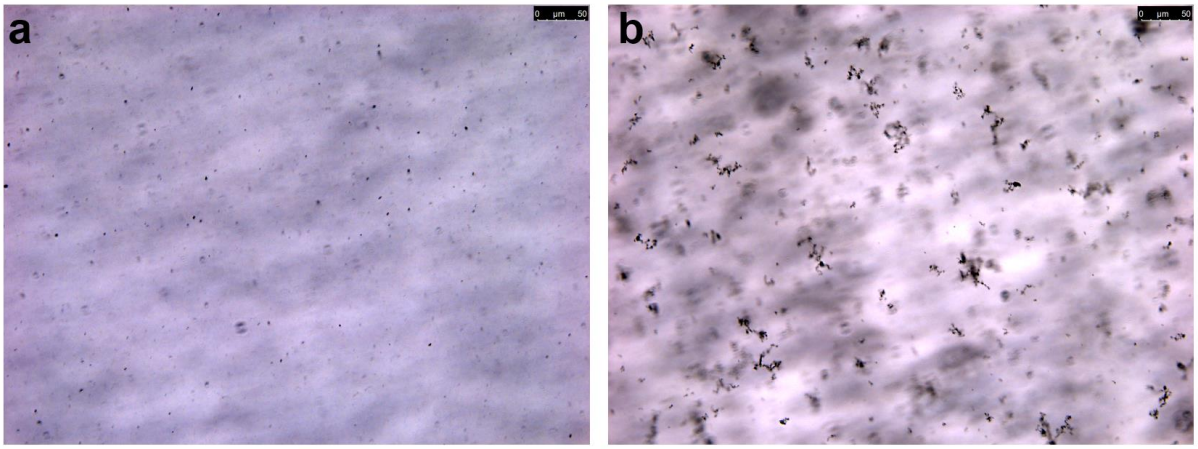

Supplementary Figure 7: **Minimisation of flake aggregation with FBS** a) Bright field microscopy images of the 6000 cycles graphene dispersed in the cell culture media and b) 6000 cycles graphene dispersed in cell culture media without FBS after 48 hours at 20x magnification.

Supplementary References

1. Torrisi, F. *et al.* Inkjet-printed graphene electronics. *ACS Nano* **6**, 2992-3006 (2012).
2. Utomo, A.T., Baker, M. & Pacek, A.W. Flow pattern, periodicity and energy dissipation in a batch rotor–stator mixer. *Chemical Engineering Research and Design* **86**, 1397-1409 (2008).
3. Sutton, G.P. & Biblarz, O. Rocket propulsion elements. (2017).
4. Paton, K.R. *et al.* Scalable production of large quantities of defect-free few-layer graphene by shear exfoliation in liquids. *Nature Materials* **13**, 624-630 (2014).
5. Bracamonte, M.V., Lacconi, G.I., Urreta, S.E. & Foa Torres, L.E.F. On the Nature of Defects in Liquid-Phase Exfoliated Graphene. *The Journal of Physical Chemistry C* **118**, 15455-15459 (2014).
6. Jackson, S.T. & Nuzzo, R.G. Determining hybridization differences for amorphous carbon from the XPS C 1s envelope. *Applied Surface Science* **90**, 195-203 (1995).
7. Al-Gaashani, R., Najjar, A., Zakaria, Y., Mansour, S. & Atieh, M.A. XPS and structural studies of high quality graphene oxide and reduced graphene oxide prepared by different chemical oxidation methods. *Ceramics International* **45**, 14439-14448 (2019).
8. Hayes, W.I., Joseph, P., Mughal, M.Z. & Papakonstantinou, P. Production of reduced graphene oxide via hydrothermal reduction in an aqueous sulphuric acid suspension and its electrochemical behaviour. *Journal of Solid State Electrochemistry* **19**, 361-380 (2015).
9. Greczynski, G., Primetzhofer, D., Lu, J. & Hultman, L. Core-level spectra and binding energies of transition metal nitrides by non-destructive x-ray photoelectron spectroscopy through capping layers. *Applied Surface Science* **396**, 347-358 (2017).
10. Sreeprasad, T.S. & Berry, V. How Do the Electrical Properties of Graphene Change with its Functionalization? *Small* **9**, 341-350 (2013).
11. Kelemen, S.R., Rose, K.D. & Kwiatek, P.J. Carbon aromaticity based on XPS II to II$*$ signal intensity. *Applied Surface Science* **64**, 167-174 (1993).
12. Stobinski, L. *et al.* Graphene oxide and reduced graphene oxide studied by the XRD, TEM and electron spectroscopy methods. *Journal of Electron Spectroscopy and Related Phenomena* **195**, 145-154 (2014).
13. Vranic, S. *et al.* Live Imaging of Label-Free Graphene Oxide Reveals Critical Factors Causing Oxidative-Stress-Mediated Cellular Responses. *ACS Nano* **12**, 1373-1389 (2018).